Analytical and Bioanalytical Chemistry (2021) 413:3955–3963
https://doi.org/10.1007/s00216-021-03347-y

RESEARCH PAPER

Sensitive colorimetric assay for the determination of alkaline phosphatase activity utilizing nanozyme based on copper nanoparticle-modified Prussian blue

Shengnan Fan[1] · Xingxing Jiang[1] · Minghui Yang[1] · Xianggui Wang[2,3]

Received: 27 February 2021 / Revised: 6 April 2021 / Accepted: 13 April 2021 / Published online: 22 April 2021

Abstract

Nanozyme based on Prussian blue nanocubes (PB NCs) loaded with copper nanoparticles (Cu@PB NCs) was synthesized. The peroxidase (POD)-like activity of Cu@PB NCs was studied and utilized for detecting the activity of alkaline phosphatase (ALP). The Cu@PB NCs possess higher POD-like activity compared with PB NCs and natural horseradish peroxidase (HRP) due to the loading of copper nanoparticles. 3,3′,5,5′-Tetramethylbenzidine (TMB) can be oxidized to oxTMB in the presence of Cu@PB NCs and H_2O_2, generating blue-colored compound, while introduction of pyrophosphate (PPi) leads to the POD-like activity of Cu@PB NCs decreased obviously. In the presence of ALP, PPi was hydrolyzed and then the POD-like activity of Cu@PB NCs was restored. So, according to the change of the POD-like activity of Cu@PB NCs, a sensitive colorimetric assay for ALP activity was reported. The limit of detection of the assay is 0.08 mU/mL, with linear range from 0.1 to 50 mU/mL. In addition, the assay was also applied for screening the inhibitors of ALP.

Keywords Nanozyme · Alkaline phosphatase · Colorimetry · Prussian blue · Inhibitor

Introduction

Alkaline phosphatase (ALP), an enzyme that can catalyze the dephosphorylation of a variety of phosphonate compounds, including nucleic acid, protein, and alkaloid, is widely distributed in human tissues, and about 90% of the ALP in serum comes from liver and bone [1, 2]. The reference ranges of serum ALP are 40–130 U/L for adult men and 35–105 U/L for adult women. The diseases associated with bone or liver are usually associated with an increased activity of ALP. Thus, ALP is an important biomarker for disease diagnosis [3–5]. Therefore, ALP assays are included in routine blood tests for diagnostic screening of patients who may have these diseases [6].

Nanozymes are nanomaterials with natural enzyme activity, which have the advantages of high stability, low cost, good stability, and easy modification [7–9]. Yan and coworkers first discovered Fe_3O_4 nanoparticles have enzymatic activity [10]. Subsequently, a variety of nanomaterials with catalytic activity has been discovered, including CeO_2 nanoparticles [11], PtFe@Fe_3O_4 [12], Ti_3C_2 nanosheets [13], and carbon nanotube [14]. Up to now, these nanozymes have been widely used in areas like antibacterial [14–16], biosensing [17–20], immunoassay [21, 22], and tumor therapy [12, 23]. Among them, Prussian blue nanoparticles (PB NPs) have attracted research interest because of their attractive properties, such as tunable size, easy of synthesis, high enzyme mimicking activities, and good biocompatibility [24–27]. In previous studies, PB has been extensively used for the preparation of electrochemical biosensors due to its high catalytic activity and selectivity towards the reduction of H_2O_2 [24].

In this work, by depositing copper nanoparticles onto PB nanocubes (PB NCs), we synthesized nanozyme, Cu@PB NCs. Utilizing the peroxidase (POD)-like activity of Cu@PB NCs, a sensitive colorimetric assay for detecting the activity of

✉ Minghui Yang
yangminghui@csu.edu.cn

✉ Xianggui Wang
wongxgui@163.com

[1] Hunan Provincial Key Laboratory of Micro & Nano Materials Interface Science, College of Chemistry and Chemical Engineering, Central South University, Changsha 410083, Hunan, China

[2] Eye Center of Xiangya Hospital, Central South University, Changsha 410011, Hunan, China

[3] Hunan Key Laboratory of Ophthalmology, Changsha 410078, Hunan, China

ALP was developed. The modification of PB NCs with copper nanoparticles improved its POD-like activity. The POD-like activity of Cu@PB NCs was utilized for catalyzing 3,3′,5,5′-tetramethylbenzidine (TMB) oxidation in the presence of H_2O_2, generating blue-colored compounds. In addition, pyrophosphate (PPi) displayed strong inhibition effect on the POD-like activity of Cu@PB NCs. But ALP can hydrolyze PPi into phosphate ions, restoring the peroxidase activity of Cu@PB NCs. So, based on the alteration of peroxidase activity of Cu@PB NCs, the detection of ALP activity was achieved.

Experimental section

Materials and apparatus

Alkaline phosphatase (ALP), glutathione (GSH), and glucose oxidase (GOx) were received from Energy Chemical (Shanghai, China). Hydrogen peroxide (30% mass fraction), hydrazine hydrate (80% mass fraction), and potassium ferricyanide ($K_3[Fe(CN)_6]$) were obtained from Sigma-Aldrich. 3,3′,5,5′-Tetramethylbenzidine (TMB) was purchased from Heowns Co., Ltd. (Tianjin, China). Sodium acetate anhydrous (CH_3COONa) and sodium pyrophosphate decahydrate ($Na_4P_2O_7$ 10 H_2O, PPi) were bought from Macklin (Shanghai, China). Fetal bovine serum used was South Africa bioind premium fetal bovine serum that was purchased from Beijing Dingguo Changsheng Biotechnology Co. Ltd. (Beijing China). All other chemicals were of analytical grade, and when used, there is no further purification.

Transmission electron microscope (TEM) images were obtained from FEI Talos × 200 microscopy (Thermo Scientific, USA). Absorption spectral data were measured with the UV-vis spectrometer (UV 2450, Shimadzu, Japan). The optical density measurements were performed at 630 nm using a BioTek Model ELx800 Microplate Reader (Shanghai, China).

Preparation of PB NCs

PB NCs were synthesized according to previous literature reported method [28]. Typically, 50% PEG aqueous solution was mixed with $K_3[Fe_{III}(CN)_6]$ aqueous solution (0.4 M, 0.5 mL) and kept at 50 °C in a water bath. And then $Fe(NO_3)_3$ aqueous solution (0.54 M, 0.5 mL) was added into the mixture under magnetic stirring. Then, the mixture was stirred for 48 h at 50 °C. By centrifugation (7600 rcf, 15 min) separated the PB NCs from the mixture. Then the nanocubes were re-dispersed in ultrapure water, centrifuged again, and freeze-dried.

The synthesis of Cu@PB NCs

Briefly, poly(ethylene glycol)methyl ether solution (Mw = 5000, 60 mL, 2 wt%), PB NCs (25 mM, 4.0 mL), and $Cu(NO_3)_2$ (1.0 mL, 0.1 M) were mixed under stirring. To this solution, hydrazine hydrate (22 μL, 80 wt%) was added and the solution was stirred for 3 min. After centrifugation (1900 rcf,15 min), the obtained product was washed three times with water as well as ethanol, and then, the product was dried at 50 °C.

Measuring the POD-like activity of Cu@PB NCs

Two hundred microliters of the HAc-NaAc buffer solution (0.2 M, pH 3.0) containing Cu@PB NCs (10 μg mL^{-1}), 400 μM TMB, and 400 μM H_2O_2 was incubated for 10 min at 35 °C. Then, the UV-vis spectra of the reaction solution were recorded. The effect of substrate concentration on the initial rate of enzymatic reaction was investigated by continuous monitoring assay. Experiments were conducted in a reaction volume of 200 μL HAc-NaAc buffer solution (0.2 M, pH 3.0) containing Cu@PB NCs (10 μg mL^{-1}), 4 mM H_2O_2 and 2 mM TMB.

PPi detection

For PPi detection, 50 μL Cu@PB NC stock solution (50 μg mL^{-1}) was added into 200 μL of HAc-NaAc buffer (0.2 M, pH 3.0) containing H_2O_2 (400 μM), TMB (400 μM), and various concentration of PPi solutions. Then, the absorbance of the solution at 630 nm was recorded in microplate reader after being incubated for 10 min at 35 °C.

Detecting the activity of ALP

Typically, 12.5 μL of different concentrations of ALP and isovolumetric of PPi (200 μM) were incubated at 35 °C for an hour. Afterward, 175 μL of HAc-NaAc buffer (0.2 M, pH 3.0) containing TMB (400 μM), H_2O_2 (400 μM), and 50 μL of Cu@PB (50 μg mL^{-1}) were added in order. After incubating at 35 °C for 10 min, the absorbance of the solution at 630 nm was recorded using microplate reader.

Detection of ALP in serum samples

ALP levels in serum were determined by standard addition method. A 12.5 μL PPi (200 μM) in HAc-NaAc buffer (0.2 M, pH 7.4) was mixed with 12.5 μL fetal calf serum and different concentrations of ALP, and then incubated at 35 °C for 10 min. The subsequent experimental procedures were performed as described above.

Results and discussion

Characterization of Cu@PB NCs

Scheme 1 shows the schematic principle of using Cu@PB NCs for ALP detection. PB NCs possess high POD-like

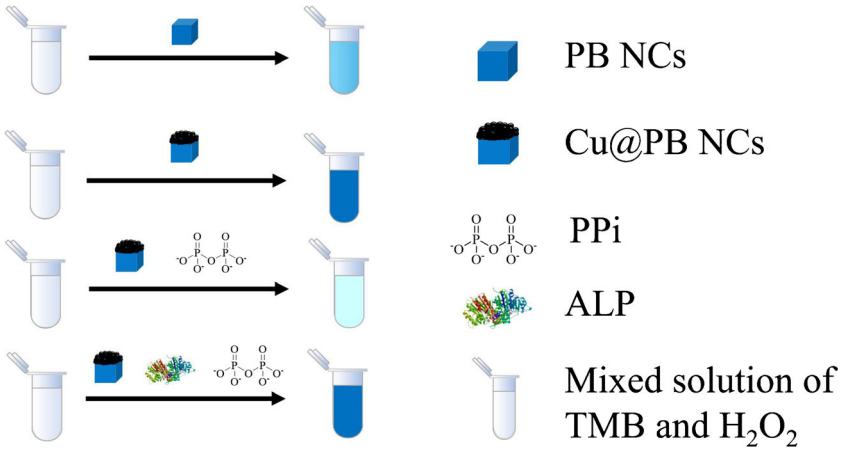

Scheme 1 Schematic illustration for the detection of ALP activity based on the peroxidase-like activity of Cu@PB NCs

activity, while Cu nanoparticles alone fail to oxidize TMB into oxTMB, which means Cu nanoparticles have no peroxidase activity. However, when Cu nanoparticles were loaded onto PB NCs, the POD-like activity of Cu@PB NCs was enhanced. In addition, the POD-like activity of Cu@PB NCs was found to be significantly suppressed by PPi, which is a natural substrate of ALP.

The PB NCs were synthesized according to literature reported method [28], and the Cu nanoparticles were loaded onto PB NCs by reducing $Cu(NO_3)_2$ with hydrazine hydrate. The morphology of the Cu@PB NCs was characterized by TEM. As shown in Fig. 1a, we can see uniform size of PB NCs with an average size of 50 ± 7 nm. Cu nanoparticles, displaying as darker dots in TEM image, are decorated onto the PB NCs. Elemental mapping data further proved that Cu nanoparticles were well-distributed over the entire PB NCs (Fig. 1b, Supplementary Information (ESM) Fig. S1).

Peroxidase-like activity of Cu@PB NCs

TMB, as a typical peroxidase substrate, was selected to characterize the POD-like activity of Cu@PB NCs. In the presence of H_2O_2, TMB can be oxidized into oxTMB with a maximum absorbance at approximately 652 nm. As shown in Fig. 2a, the absorption intensity of the TMB/H_2O_2/Cu@PB NCs system has the maximum value at 652 nm. Besides, Fig. 2b shows that Cu nanoparticles alone has no peroxidase activity, and PB NCs have a lower POD-like activity than Cu@PB NCs (ESM Fig. S2). Moreover, with the increase of the ratio of Cu to PB NCs, the POD-like activity of Cu@PB NCs was also increased (ESM Fig. S3). However, in the presence of PPi, the absorption intensity was decreased. Especially, the absorption intensity decreased more significantly for Cu@PB NCs compare to PB NCs (Fig. 2b, ESM Fig. S2a). Due to the binding between PPi and Cu, PPi can be adsorbed onto the surface of Cu@PB NCs which resulted in the greatly decrease of the

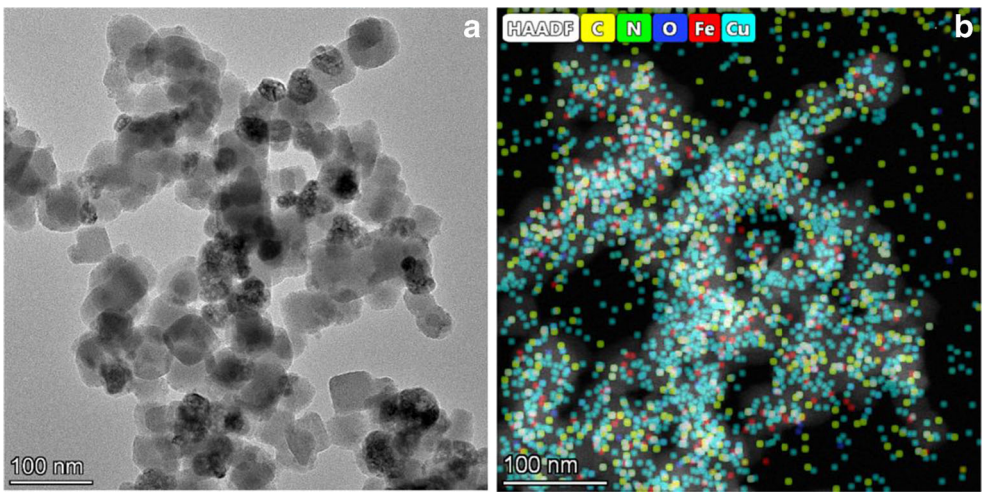

Fig. 1 **a** TEM image of Cu@PB NCs. **b** Elemental mapping images of Cu@PB NCs (C, N, Fe, Cu, O)

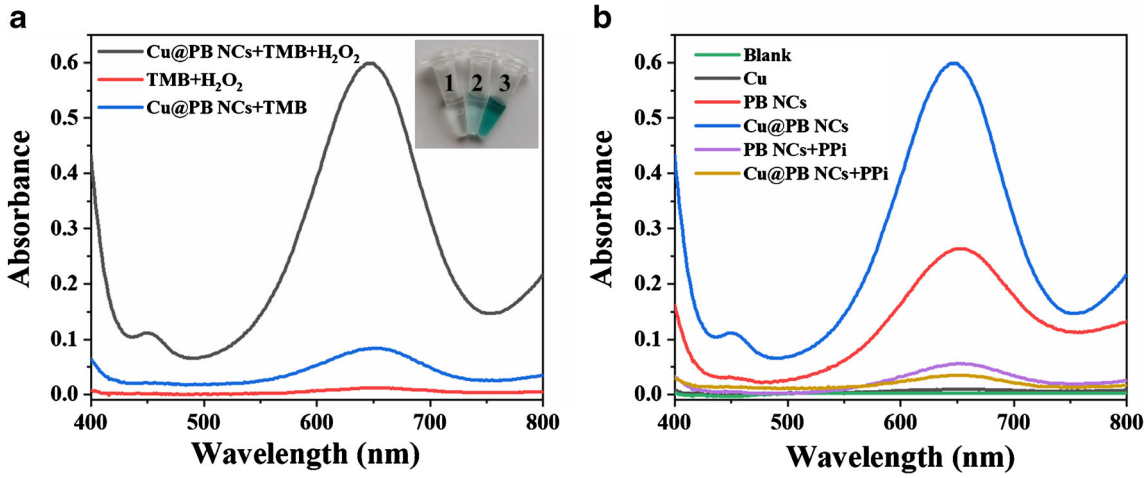

Fig. 2 **a** The absorbance spectra of different reaction systems: (1) TMB/H_2O_2, (2) TMB/Cu@PB NCs, and (3) TMB/H_2O_2/Cu@PB NCs in HAc-NaAc buffer solution (0.2 M, pH 3.0) after incubating at 35 °C for 10 min. The insets correspond to the color variations of the different systems. **b** UV-vis spectra of TMB/H_2O_2 system with different nanomaterials

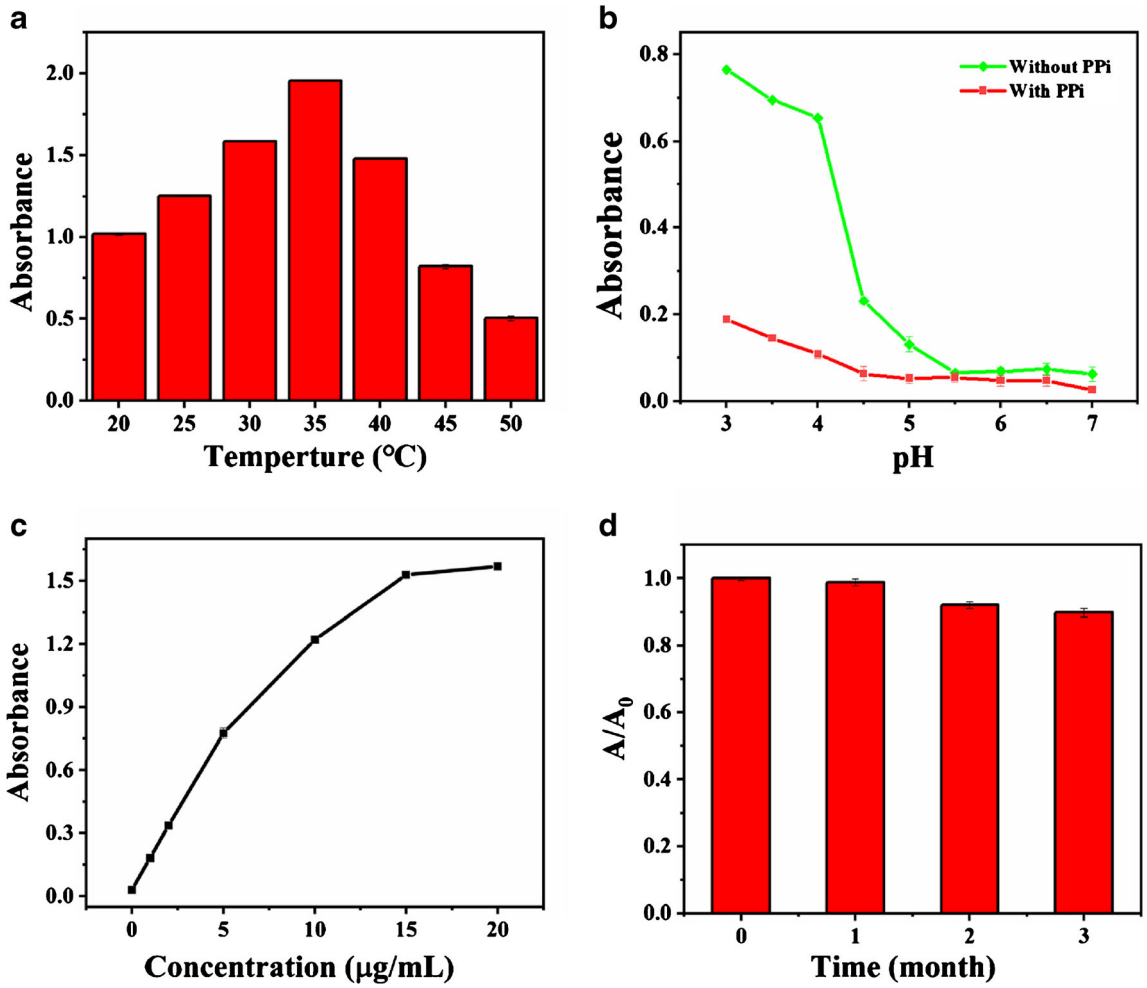

Fig. 3 **a** The POD-like activity of Cu@PB NCs varies with temperature. **b** pH-dependent absorption intensity of TMB/H_2O_2/Cu@PB NCs system in the absence or presence of PPi. **c** The absorption intensity of TMB/H_2O_2/Cu@PB NCs system varies with the concentration of Cu@PB NCs. **d** By storing the Cu@PB NCs at room temperature for 3 months to determinate the stability of its POD-like activity. All data were measured at 630 nm using microplate reader. The error bar represents the standard deviation of three independent measurements

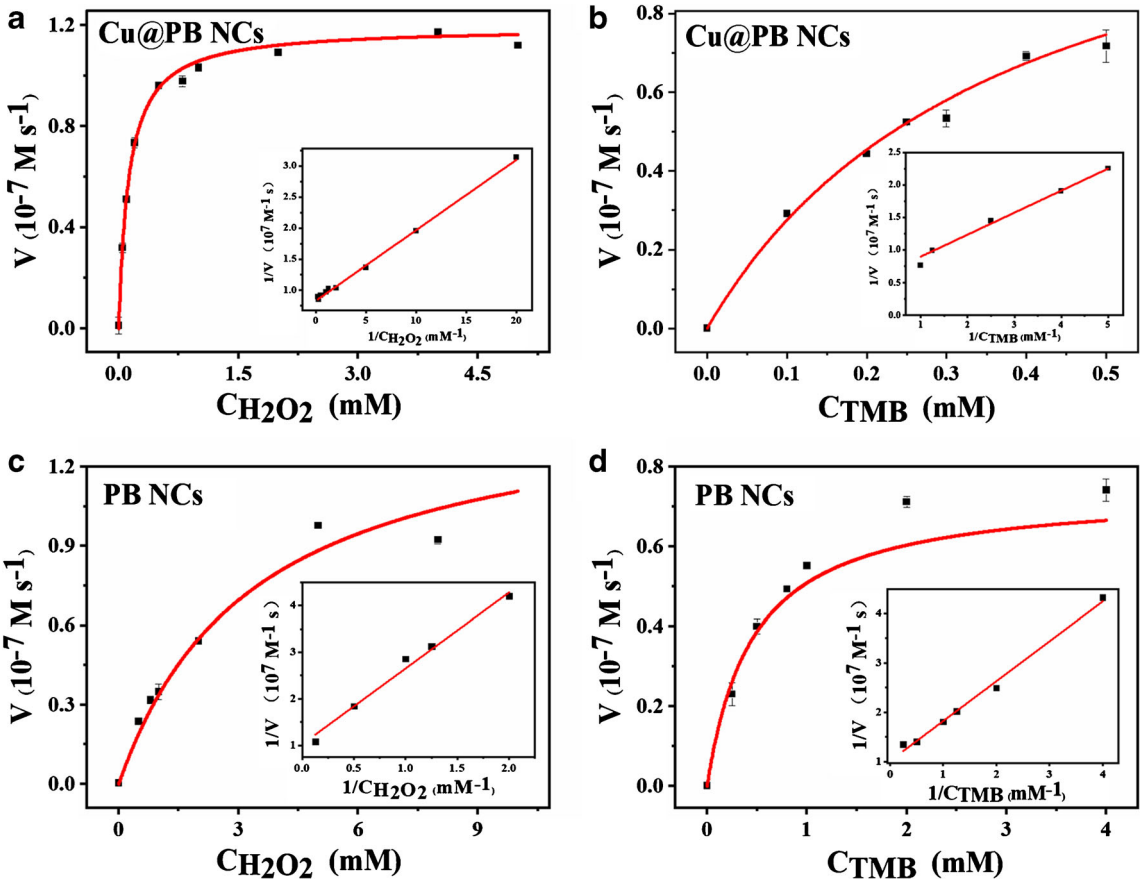

Fig. 4 The kinetic and double-reciprocal curves of Cu@PB NCs (**a**, **b**) and PB NCs (**c**, **d**) with H_2O_2 and TMB as substrates. The error bar represents the standard deviation of three independent measurements

POD-like activity of Cu@PB NCs [29, 30]. In consideration of the effect of PPi on the peroxidase activity of the Cu@PB NCs, we finally chose the material with copper and PB molar ratio of 10 to 1 for subsequent experiments (ESM Fig. S3).

The catalytic performance of nanozymes is influenced by many factors, including temperature and pH value. In this work, we studied the optimum pH, temperature, and Cu@PB NCs concentration. As shown in Fig. 3a and b, the optimum pH and temperature were 3.0 and 35 °C, respectively. With the increased concentration of Cu@PB NCs, the absorbance intensity increased and gradually decreased after 10 μg/mL. Excessive concentration of Cu@PB NCs would lead to a too violent and rapid reaction and a decrease of the absorbance at 652 nm. So the Cu@PB NCs concentration of 10 μg mL^{-1} was selected (Fig. 3c). The long-term storage stability of enzymes is an important parameter. After stored at room temperature for 3 months, the Cu@PB NCs still maintained 90% of its original activity (Fig. 3d). In addition, compared with the freshly prepared Cu@PB NCs, the Km of Cu@PB NCs to TMB decreased to 92.3% and the Vmax decreased to 50% after 3 months of storage. The Km of Cu@PB NCs to H_2O_2 is reduced to 42.2%, and Vmax is reduced to 32.2%.

Kinetic experiments

To fully demonstrate the good POD-like activity of Cu@PB NCs, kinetic experiments were conducted to compare the Km and Vmax of Cu@PB NCs, PB NCs and HRP with TMB and H_2O_2 as their catalytic substrates (Fig. 4). Lineweaver-Burk double-reciprocal plot were used to obtain Km and Vmax, and the results are recorded on Table 1. Km and Vmax represented the affinity of the substrates to enzymes and the turnover

Table 1 The comparison of the kinetic parameters of Cu@PB NCs, PB NCs, and HRP

Materials	Substrate	Km/mM	Vmax/ 10^{-7} M s^{-1}	T/ °C
Cu@PB NCs	TMB	0.60±0.01	1.79±0.09	25
	H_2O_2	0.14±0.01	1.20±0.01	
PB NCs	TMB	0.80±0.03	0.99±0.04	
	H_2O_2	1.58±0.07	0.97±0.05	
HRP	TMB	0.43	1.0	40
	H_2O_2	3.7	0.8	

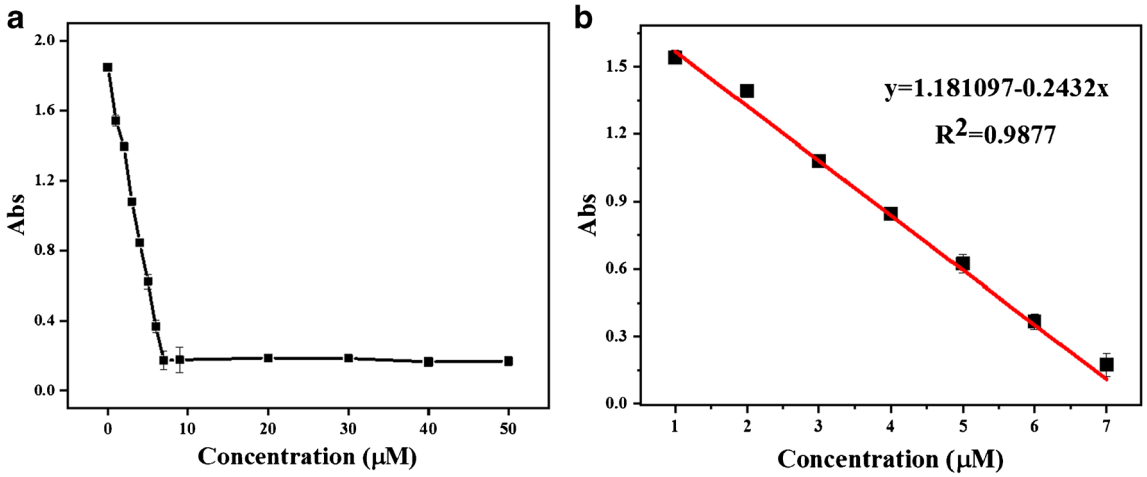

Fig. 5 **a** The absorbance intensity changes of TMB/H_2O_2/PPi/Cu@PB NCs system against different concentration of PPi at 630 nm. **b** Linear response range between PPi concentration and absorbance intensity. The error bar represents the standard deviation of three independent measurements

number of an enzyme, respectively [31]. Furthermore, a small Km and a large Vmax indicate that the enzyme has high affinity and conversion efficiency to the substrate. To TMB substrate, compared to HRP, Cu@PB NCs had stronger affinity and higher catalytic efficiency. As for H_2O_2 substrate, compared to HRP, Cu@PB NCs have a particularly small Km. All these results indicated that Cu nanoparticles played a pivotal role in increasing the affinities of the substrates to Cu@PB NCs and provided more catalytic sites for H_2O_2 decomposition, which enhanced the catalytic activity of Cu@PB NCs. The loading of Cu nanoparticles increased the affinity of Cu@PB NCs to H_2O_2 by about 11 times and to TMB by about 1.3 times compared to PB NCs.

The mechanism of catalytic properties of Cu@PB NCs

Under acidic conditions, PB can be oxidized to Berlin green (BG) or Prussian yellow (PY) by H_2O_2, and the redox potential of PY/BG is between the redox potential of oxTMB/TMB and H_2O_2/H_2O; as a result, electrons can be easily transformed from TMB to H_2O_2 by PY/BG [26]. The doping of copper leads to a decrease in zeta potential of PB NCs (ESM Fig. S4). From literature reports, we know the pKa of TMB is about 4.2; thus, TMB is positively charged in acidic medium with a pH less than 4.2 [32]. Based on the above experimental facts, we speculate that under optimized reaction conditions, PB NCs with negative zeta potential can adsorb TMB and promote electron transfer. The

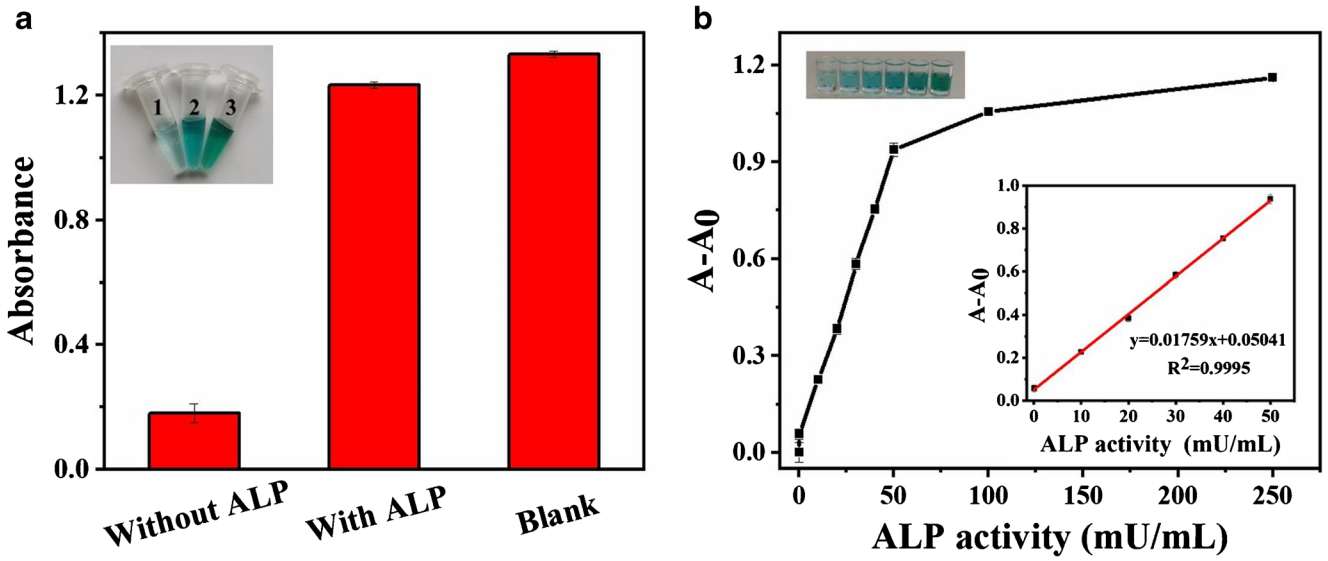

Fig. 6 **a** Feasibility of the assay for ALP detection. **b** The absorption changes of the assay to different activity of ALP. The inset shows corresponding color variation of the assay to ALP and linear range of the assay to different activity of ALP

Table 2 Comparison of several previously reported ALP sensors

Analytical method	Biosensing materials	Detection limit (U/L)	Linear range(U/L)	Reference
SERS	AMNS	0.04	0.4–20	[34]
Colorimetry	AuNC-TMB-H_2O_2/PPi	0.005	0.01–4	[32]
Fluorescent	MoS_2 QDs	0.1	0.1–5	[35]
Photothermal	MnO_2 nanosheet	0.1	0–10	[3]
Colorimetry	In situ formed Ag NPs	0.037	0.15–5	[36]
Electrochemical	Aminoferrocene	1.48	200–100	[37]
Colorimetry	Cu@PB NCs	0.08	0.1–50	This work

modification of Cu nanoparticles provides more active sites for H_2O_2, which leads to a significant increase in the affinity of the composites for H_2O_2, thus enhancing the peroxidase activity of the Cu@PB NCs.

Detection of PPi

As indicated above, Cu@PB NCs can facilitate the electron transfer between TMB and H_2O_2, generating oxTMB—a blue-colored compound. Upon addition PPi, PPi has a strong binding with copper ion on the surface of Cu@PB, so that the active sites on the surface of Cu@PB are blocked and electron transfer is hindered [29, 30]. Based on mentioned above, we measured the color change of TMB/H_2O_2/Cu@PB NCs/PPi system to measure different concentration of PPi. We firstly measured the incubation time between PPi and Cu@PB NCs, then we found PPi can inhibit the activity of Cu@PB NCs quickly (ESM Fig. S5a). As shown in Fig. 5, the colorimetric responses decreased with the increasing concentration of PPi. Besides, a good linear correlation can be established between absorption intensity and the concentration of PPi over a range of 1 to 7 μM with a regression equation of $A_{630} = 1.1811 – 0.2438$ [PPi]/μM. Based on 3σ/s, the detection limit is calculated to be 0.245 μM.

Quantitative detection of ALP activity by Cu@PB NCs

Since PPi is the natural substrate for ALP, through hydrolysis of PPi by ALP, we can measure ALP activity accordingly. Various activity of ALP was incubated with 100 μM PPi, and then the amount of PPi left was tested. The POD-like activity of Cu@PB NCs was almost fully recovered in the presence of ALP (Fig. 6a), indicating the PPi were almost completely hydrolyzed. The incubation time between PPi and ALP was optimized and 1 h was selected as the optimum incubation time (ESM Fig. S5b). As shown in Fig. 6b, the absorbance intensity of oxTMB increased gradually with the increase of concentration of ALP, and ALP can be detected in the linear range from 0.1 to 50 mU mL^{-1}. The LOD of this assay is 0.08 mU/mL ($S/N = 3$). Besides, the linear range and LOD of this assay utilizing Cu@PB NCs are better than literature reported methods (Table 2).

Selectivity of the assay

To test the selectivity of this assay, we then measured the influence of other biomolecules present in the serum sample on the performance of the assay. We chose common biomolecules, including glucose (Glu), dopamine (DA), bovine serum albumin (BSA), glutathione (GSH), lactate

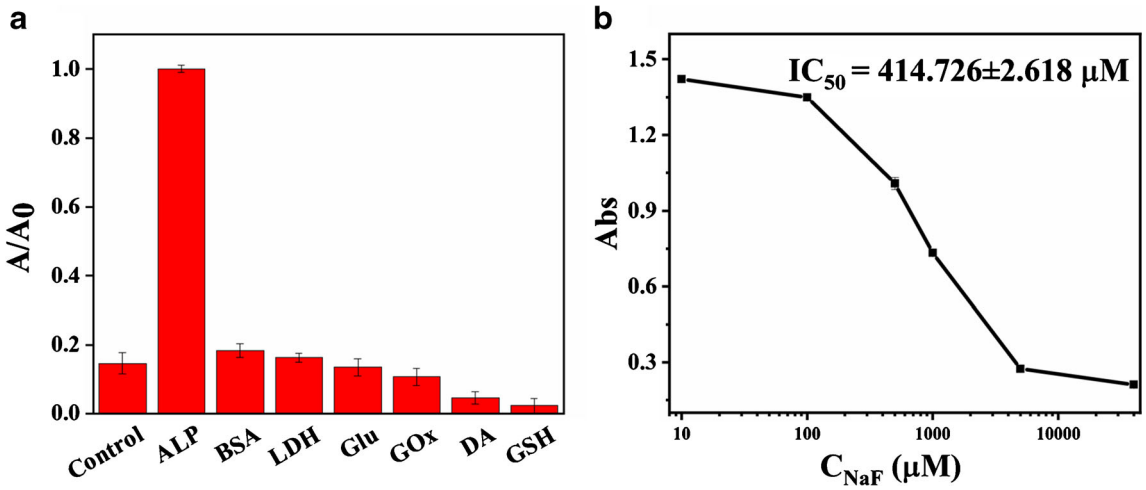

Fig. 7 **a** Selectivity of the assay to different biomolecules. **b** Effects of different concentrations of NaF on ALP activity

Table 3 The detection of ALP activity in serum samples

Sample	Added (mU/mL)	Found (mU/mL)	Recovery (%)	RSD (%)
1	0	7.69 ± 1.30	/	4.93
2	15	22.62 ± 0.10	99.55	0.29
3	20	27.30 ± 0.12	98.07	0.33
4	40	48.36 ± 1.95	101.67	3.57

dehydrogenase (LDH), and glucose oxidase (GOx). The final concentration of biomolecules was 2 mg mL^{-1} except for LDH, which is 100 mU mL^{-1}. As shown in Fig. 7a, compared to the response of the assay to ALP, these molecules did not interfere with the ALP detection. It is worth noting that DA and GSH resulted in a significant decrease in absorbance compared to the blank, which is because DA and GSH are reductive substance that can induce the reduction of oxTMB.

Detection of ALP inhibition

NaF was chosen as model drug to test the feasibility of the assay for screening ALP inhibitors since NaF has been proved that can inhibit ALP activity [33]. As shown in Fig. 7b, a gradual increase in NaF concentration was accompanied by a decrease in the absorbance intensity, which means the activity of ALP was inhibited. The relationship between the concentration of inhibitor and enzyme activity shows an S-shaped curve with the IC_{50} (inhibitory concentration of 50% of the enzyme activity) value of 414.7 ± 2.6 μM, which suggests the assay can be applied to screen potential ALP inhibitors.

Detection of ALP in serum sample

To verify the reliability of the assay, detection of ALP activity in biological samples was performed. Standard addition method was used to detect ALP in fetal bovine serum. As shown in Table 3, ALP was added into serum with activity of 15, 20, and 40 mU/mL, respectively. The recoveries were between 98.07 and 101.67%, and the relative standard deviation (RSD) was less than 5%. Therefore, Cu@PB NCs as a peroxidase mimic has potential application in the clinical detection of ALP.

Conclusions

In this work, we synthesized Prussian blue nanocube loaded with copper nanoparticles (Cu@PB NCs) as a peroxidase mimic. The POD-like activity of PB NCs was improved through the loading of copper nanoparticles. Based on the high POD-like activity of Cu@PB NCs, a sensitive colorimetric assay was constructed and applied to detect ALP activity. The detection of ALP activity was due to the suppression of the POD-like activity of Cu@PB NCs by PPi and hydrolysis of PPi by ALP. This assay has the advantages of high selectivity and wide linear response range for ALP detection, and can be used to screen potential inhibitors of ALP. Compared with single PB NCs, the synthesized Cu@PB NCs has significantly improved catalytic activity, which provided a new way for enhancing the catalytic activity of nanozymes.

Supplementary Information The online version contains supplementary material available at https://doi.org/10.1007/s00216-021-03347-y.

Funding The authors thank the Hunan Provincial Science and Technology Plan Project, China (No. 2019TP1001) and Innovation-Driven Project of Central South University (2020CX002) for the financial support of this work.

Declarations

Ethics approval All experiments were in accordance with the guidelines of the National Institute of Health, China, and approved by the Institutional Ethical Committee (IEC) of the Second Xiangya Hospital that attached to Central South University.

Competing interests The authors declare no competing interests.

References

1. Stinghen ST, Moura JF, Zancanella P, Rodrigues GA, Pianovski MA, Lalli E, et al. Specific immunoassays for placental alkaline phosphatase as a tumor marker. J Biomed Biotechnol. 2006;2006:056087.
2. Loke SC, Tan AWK, Dalan R, Leow MK-S. Pre-operative serum alkaline phosphatase as a predictor for hypocalcemia post-parathyroid adenectomy. Int J Med Sci. 2012;9(7):611–6.
3. Liu X, Zou L, Yang X, Wang Q, Zheng Y, Geng X, et al. Point-of-care assay of alkaline phosphatase enzymatic activity using a thermometer or temperature discoloration sticker as readout. Anal Chem. 2019;91(12):7943–9.
4. Zhang L, Nie J, Wang H, Yang J, Wang B, Zhang Y, et al. Instrument-free quantitative detection of alkaline phosphatase using paper-based devices. Anal Methods. 2017;9(22):3375–9.
5. Peters E, Masereeuw R, Pickkers P. The potential of alkaline phosphatase as a treatment for sepsis-associated acute kidney injury. Nephron Clin Pract. 2014;127(1–4):144–8.
6. Jiang Y, Li X, Walt DR. Single-molecule analysis determines isozymes of human alkaline phosphatase in serum. Angew Chem Int Ed. 2020;59(41):18010–5.
7. Huang Y, Ren J, Qu X. Nanozymes: classification, catalytic mechanisms, activity regulation, and applications. Chem Rev. 2019;119(6):4357–412.
8. Zhang T, Xing Y, Song Y, Gu Y, Yan X, Lu N, et al. AuPt/MOF-graphene: a synergistic catalyst with surprisingly high peroxidase-like activity and its application for H2O2 detection. Anal Chem. 2019;91(16):10589–95.
9. Zhang J, Wu S, Lu X, Wu P, Liu J. Manganese as a catalytic mediator for photo-oxidation and breaking the pH limitation of nanozymes. Nano Lett. 2019;19(5):3214–20.

10. Gao L, Zhuang J, Nie L, Zhang J, Zhang Y, Gu N, et al. Intrinsic peroxidase-like activity of ferromagnetic nanoparticles. Nat Nanotechnol. 2007;2(9):577–83.
11. Asati A, Santra S, Kaittanis C, Nath S, Perez JM. Oxidase-like activity of polymer-coated cerium oxide nanoparticles. Angew Chem Int Ed. 2009;48(13):2308–12.
12. Li S, Shang L, Xu B, Wang S, Gu K, Wu Q, et al. A nanozyme with photo-enhanced dual enzyme-like activities for deep pancreatic cancer therapy. Angew Chem Int Ed. 2019;58(36):12624–31.
13. Zhu X, Fan L, Wang S, Lei C, Huang Y, Nie Z, et al. Phospholipid-tailored titanium carbide nanosheets as a novel fluorescent nanoprobe for activity assay and imaging of phospholipase D. Anal Chem. 2018;90(11):6742–8.
14. Wang H, Li P, Yu D, Zhang Y, Wang Z, Liu C, et al. Unraveling the enzymatic activity of oxygenated carbon nanotubes and their application in the treatment of bacterial infections. Nano Lett. 2018;18(6):3344–51.
15. Niu J, Sun Y, Wang F, Zhao C, Ren J, Qu X. Photomodulated nanozyme used for a gram-selective antimicrobial. Chem Mater. 2018;30(20):7027–33.
16. Jiang X, Liu K, Li Q, Liu M, Yang M, Chen X. B-Doped core–shell Fe@BC nanozymes: active site identification and bacterial inhibition. Chem Commun. 2021;57(13):1623–6.
17. Li S, Ma X, Pang C, Wang M, Yin G, Xu Z, et al. Novel chloramphenicol sensor based on aggregation-induced electrochemiluminescence and nanozyme amplification. Biosens Bioelectron. 2021;176:112944.
18. Zhu Y, Wu J, Han L, Wang X, Li W, Guo H, et al. Nanozyme sensor arrays based on heteroatom-doped graphene for detecting pesticides. Anal Chem. 2020;92(11):7444–52.
19. Wu T, Ma Z, Li P, Lu Q, Liu M, Li H, et al. Bifunctional colorimetric biosensors via regulation of the dual nanoenzyme activity of carbonized FeCo-ZIF. Sensors Actuators B Chem. 2019;290:357–63.
20. Fang A, Chen H, Li H, Liu M, Zhang Y, Yao S. Glutathione regulation-based dual-functional upconversion sensing-platform for acetylcholinesterase activity and cadmium ions. Biosens Bioelectron. 2017;87:545–51.
21. Tian B, Zhao L, Li R, Zhai T, Zhang N, Duan Z, et al. Electrochemical immunoassay of endothelin-1 based on a Fenton-type reaction using Cu(II)-containing nanocomposites as nanozymes. Anal Chem. 2020;92(24):15916–26.
22. Yu L, Li M, Kang Q, Fu L, Zou G, Shen D. Bovine serum albumin-stabilized silver nanoclusters with anodic electrochemiluminescence peak at 904 nm in aqueous medium and applications in spectrum-resolved multiplexing immunoassay. Biosens Bioelectron. 2020;176:112934.
23. Dong S, Dong Y, Jia T, Liu S, Liu J, Yang D, et al. GSH-depleted nanozymes with hyperthermia-enhanced dual enzyme-mimic activities for tumor nanocatalytic therapy. Adv Mater. 2020;32(42):e2002439.
24. Gao X, Wang Q, Cheng C, Lin S, Lin T, Liu C, et al. The application of Prussian blue nanoparticles in tumor diagnosis and treatment. Sensors. 2020;20(23).
25. Komkova MA, Ibragimova OA, Karyakina EE, Karyakin AA. Catalytic pathway of nanozyme "artificial peroxidase" with 100-fold greater bimolecular rate constants compared to those of the enzyme. J Phys Chem Lett. 2021;12(1):171–6.
26. Zhang W, Hu S, Yin JJ, He W, Lu W, Ma M, et al. Prussian blue nanoparticles as multienzyme mimetics and reactive oxygen species scavengers. J Am Chem Soc. 2016;138(18):5860–5.
27. Zhang W, Zhang Y, Chen Y, Li S, Gu N, Hu S, et al. Prussian blue modified ferritin as peroxidase mimetics and its applications in biological detection. J Nanosci Nanotechnol. 2013;13(1):60–7.
28. Shiba F, Mameuda U, Tatejima S, Okawa Y. Synthesis of uniform Prussian blue nanoparticles by a polyol process using a polyethylene glycol aqueous solution. RSC Adv. 2019;9(59):34589–94.
29. Guo L, Chen D, Yang M. DNA-templated silver nanoclusters for fluorometric determination of the activity and inhibition of alkaline phosphatase. Microchim Acta. 2017;184(7):2165–70.
30. Li X, Luo J, Jiang X, Yang M, Rasooly A. Gold nanocluster-europium(III) ratiometric fluorescence assay for dipicolinic acid. Microchim Acta. 2021;188(1):26.
31. Lv J, Wang S, Zhang C, Lin Y, Fu Y, Li M. ATP induced alteration in the peroxidase-like properties of hollow Prussian blue nanocubes: a platform for alkaline phosphatase detection. Analyst. 2020;145(14):5032–40.
32. Chen C, Zhao D, Jiang Y, Ni P, Zhang C, Wang B, et al. Logically regulating peroxidase-like activity of gold nanoclusters for sensing phosphate-containing metabolites and alkaline phosphatase activity. Anal Chem. 2019;91(23):15017–24.
33. Shen C, Li X, Rasooly A, Guo L, Zhang K, Yang M. A single electrochemical biosensor for detecting the activity and inhibition of both protein kinase and alkaline phosphatase based on phosphate ions induced deposition of redox precipitates. Biosens Bioelectron. 2016;85:220–5.
34. Liu H, Wei L, Hua J, Chen D, Meng H, Li Z, et al. Enzyme activity-modulated etching of gold nanobipyramids@MnO2 nanoparticles for ALP assay using surface-enhanced Raman spectroscopy. Nanoscale. 2020;12(18):10390–8.
35. Zhong Y, Xue F, Wei P, Li R, Cao C, Yi T. Water-soluble MoS2 quantum dots for facile and sensitive fluorescence sensing of alkaline phosphatase activity in serum and live cells based on the inner filter effect. Nanoscale. 2018;10(45):21298–306.
36. Song H, Li Z, Peng Y, Li X, Xu X, Pan J, et al. Enzyme-triggered in situ formation of Ag nanoparticles with oxidase-mimicking activity for amplified detection of alkaline phosphatase activity. Analyst. 2019;144(7):2416–22.
37. Wang W, Lu J, Hao L, Yang H, Song X, Si F. Electrochemical detection of alkaline phosphatase activity through enzyme-catalyzed reaction using aminoferrocene as an electroactive probe. Anal Bioanal Chem. 2021;413(7):1827–36.